CHEMICAL ENGINEERING TRANSACTIONS
VOL. 67, 2018
A publication of AIDIC
The Italian Association of Chemical Engineering
Online at www.aidic.it/cet
Guest Editors: Valerio Cozzani, Bruno Fabiano, Davide Manca
Copyright © 2018, AIDIC Servizi S.r.l.
ISBN 978-88-95608-64-8; **ISSN** 2283-9216

Tomographic and Scattering Based Methods for Damage Detection on Atmospheric Storage Tanks

Marco Messina[a,*], Luca De Marchi[b], Nicola Testoni[a], Valerio Cozzani[c], Alessandro Marzani[b]

[a]Department of Civil, Chemical, Environmental and Materials Engineering, DICAM, University of Bologna, Viale Del Risorgimento 2, 40136, Bologna, Italy
[b]Department of Electric, Electronic, and Information Engineering "Guglielmo Marconi", DEI, University of Bologna, Viale Del Risorgimento 2, 40136, Bologna, Italy
[c]Department of Civil, Chemical, Environmental and Materials Engineering, DICAM, University of Bologna, Via Terracina 28, 40131, Bologna, Italy
marco.messina4@unibo.it

Structural Health Monitoring (SHM) systems based on ultrasonic guided waves and sensors permanently installed on structures have the potential to decrease the maintenance costs and reduce the risk of failures of critical components in a chemical plant. Such systems, in fact, can check the health status of the structure, prompting maintenance interventions only when needed and not at prescribed intervals. Moreover, they can be used on a real time basis or activated in remote for extemporary checks. The monitoring process consists in two main steps: (i) detection of waves at specific positions via proper sensor-node networks and (ii) post processing the gathered signals with the aim of assessing the structural integrity. The aim of this paper is to compare two post processing techniques, namely (i) the tomography (TM) and (ii) the wave scattering method (WSM), commonly used for damage detection and localization. As a test case, guided waves propagating in small portion of a steel atmospheric tank mantle have been simulated via Finite Element and used to test the ability of both algorithms to detect and locate the position of the damage with respect to its severity and the adopted number of sensors.

1. Introduction

The health status of thin and large metallic structures can be efficiently assessed by ultrasonic guided waves (GWs) (Li and Zhou, 2016) thanks to their minimum activation energy and low attenuation. As reported by (Maheri and Abdollahi A., 2013), although a lifespan of a ground steel storage tank is of the order of 40 years, failures due to corrosion have been reported after only 3 years in service. Steel storage tanks containing liquids are susceptible to corrosion from the inside, which could cause a reduction of the walls or roof thickness, generating imperfections and in turn decreasing significantly the critical buckling load of the structure (Shokrzadeh and Sohrabi, 2016). To assess the health status of such structures, array of piezoelectric sensors can be used to excite and sense GWs, and ad-hoc signal processing methodologies used to analyse the acquired signals. The two processing techniques under investigation are (i) the so-called tomography (TM) and (ii) the wave scattering method (WSM). In this work, a small portion of a steel tank and a high number of sensors have been considered to test the performances of both approaches. The considered scenario allows to limit the computational time (small portion of the tank) for generating the signals and to test the imaging performance vs the number of actuator-sensor pairs.

2. TM and WSM operating principles

The key operating principles of TM consists in comparing the GW signal of an actuator-sensor pair detected on a structure in pristine condition, with the one detected after a damage has occurred. Differences in the two signals are used to denote the presence of the defect in the actuator-sensor path. Increasing the number of actuators and sensors, and so the wave paths, and combining the indicators of all paths, allow to detect and

locate the defect. The 'Reconstruction Algorithm for Probabilistic Inspection of Damage' (RAPID) is the algorithm used in this work for localizing the damaged area (Tabatabaeipour et al., 2014). The basic principle of WSM consists in exciting a guided wave from an actuator and measuring the time of flight (ToF) of the wave traveling along the direct path actuator-sensor, as well as the ToF related to the wave path actuator-defect-sensor. The ToF of the scattered wave can be converted in a distance of propagation, once the speed of the wave or its dispersion curve is known, and then used to feed triangulation schemes aimed at revealing the presence of the defect, as well as locating the defect position.

3. Signal generation and imaging methods

In this work, the Finite Element Method has been used to compute the GW signals propagating in the tank mantle. Given the very low mantle thickness vs curvature ratio, a flat plate with an edge length of 0.3 m and 10 mm thickness made of A36 steel, (Young's modulus E = 200 GPa; Poisson ratio ν = 0.26 and density ρ = 7800 kg/m^3), has been considered. To model the corrosion, a square notch of size L_d = 17.50 mm and depth h_d with its center located in position (x_d, y_d, z_{lower}) on the opposite side of the plate used for collecting the signals, has been used. Initial conditions are prescribed as zero displacement and zero velocity fields; whereas boundary conditions are low-reflecting along the plate edges.
The plate geometry is discretized with Finite Elements having maximum dimension L_e less than 1/8 of the minimum expected wave length (Duczek et al., 2014), which correspond to the A_0 wave. For evaluating the minimum A_0 wave length, the dispersion curves of the A36 steel plate 10 mm thick have been determined using the tool GUIGUW (Bocchini at al., 2011) and shown in Figure 1. The time adopted in the Finite Element simulations satisfies the Courant Friedrichs Levy (CFL) condition with a CFL value of 0.25, based on the group velocity of the S_0 wave.
A circular array with radius R_a = 69.81 mm of sixteen (16) sensors is positioned on the upper surface of the plate around the notch. Since it is necessary to simulate each sensor actuation, both for the pristine and the damaged plate, the dimension of the plate, the initial number of sensor and its radius are kept small to reduce the computational burden. The actuator is modelled with a spatially constant surface pressure $p(x,y,z_{upper},t) = p(t)$ over a circular area of 16 mm radius. This value assures that at least two elements per radius are subject to the load. The pressure time variation is a Hanning modulated sine burst at 50 kHz and 4 cycles.
Simulations data are computed for a structure without corrosion and with corrosion for different values of damage depths and positions, h_d and (x_d,y_d,z_{lower}), respectively. The term baseline is used for the data collected from the pristine structure, whereas the term current is used for the data with corrosion. MATLAB (The MathWorks Inc., 2017) has been used to post-process all the signals.

3.1 TM based imaging

For each transmitter i and receiver j a signal difference coefficient value (SDC_{ij}) between the baseline $B_{ij}(t)$ and current state $D_{ij}(t)$ signals can be constructed (Tabatabaeipour et al., 2014):

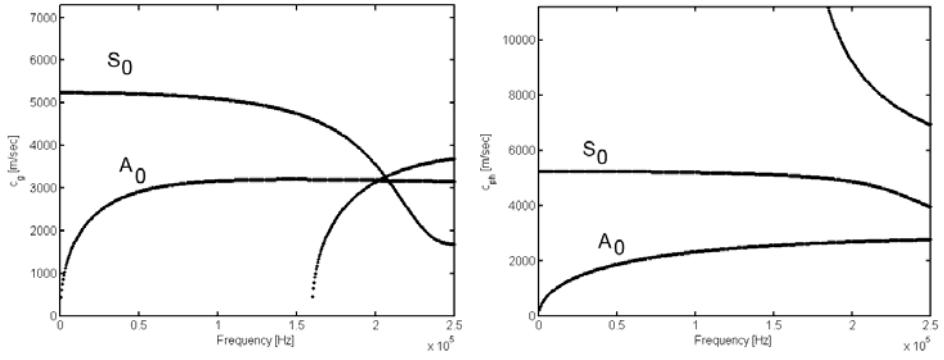

(a) *(b)*

Figure 1: GUIGUW (a) group velocity and (b) phase velocity dispersion curves for A36 steel plate 10 mm thick.

$$SDC_{ij} = 1 - \frac{\sum_{k=1}^{n}\left(B_{ij}(t_k) - \overline{B_{ij}}\right)\left(D_{ij}(t_k) - \overline{D_{ij}}\right)}{\sqrt{\sum_{k=1}^{n}\left(B_{ij}(t_k) - \overline{B_{ij}}\right)^2 \sum_{k=1}^{n}\left(D_{ij}(t_k) - \overline{D_{ij}}\right)^2}} \quad (1)$$

where k runs through all the n time steps recorded, and an overbar denotes the mean average. This coefficient is a measure of the difference between the two structures and thus it can be used as an indicator of the presence of damage between the pair ij. Assuming a priori spatial probability distribution $s_{ij}(x,y)$ as an ellipsis, with foci the transmitter i and the receiver j, a damage presence probability $P(x,y)$ can be defined as:

$$P(x,y) = \sum_{i=1}^{n}\sum_{j=1,j\neq i}^{n} SDC_{ij}s_{ij} \quad (2)$$

where n is the total number of sensors used.

3.2 WSM based imaging

The procedure relies on the accurate estimation of the distance of propagation of the scattered waves from a defect (Monaco et al., 2016). As preliminary computation, for each pair actuator A and receiver R, the maximum of each Hilbert transformed signal is found: $t_{A,0}$ and $t_{R,0}$, which allows to define a time gated envelope $e_{AR}(t)$ on the received signal. For a generic point P_i on the upper surface of the plate, the distances from the receiver R and transmitter A is computed as:

$$d(P_i) = |\overrightarrow{P_A P_i}| + |\overrightarrow{P_R P_i}| \quad (3)$$

When divided by the group velocity $c_g(f_0)$, it gives the time of flight $t_i = d(d_i)/c_g(f_0)$. A probability to have recorded a reflection between the direct path AR and the first reflection, that happens only in presence of defect, is directly related to a damage index $DI(x,y)$ defined as (De Marchi et al., 2013):

$$DI(x,y) = \sum_{A=1}^{n}\sum_{R=1,R\neq A}^{n}\left[e_{AR}^{D}\left(t_{A,0} + \frac{dP_i}{c_g(f_0)}\right) - e_{AR}^{B}\left(t_{A,0} + \frac{dP_i}{c_g(f_0)}\right)\right] \quad (4)$$

where the subscripts D and B are related to the current and baseline signals.

4. Results

4.1 Tomography and Wave Scattering Method

For the first test case the notch has been positioned at (x_d = 52.49; y_d = 0.00) mm (damage 1). Figure 2 shows the normalized damage probability $P(x,y)$ for TM and damage index $DI(x,y)$ for WSM for h_d equal to 3 mm. For both approaches 16, 8 and 4 sensors have been considered. For the second position of the notch at (x_d = 87.48; y_d = -17.50) mm (damage 2). Figure 3 shows $P(x,y)$ and $DI(x,y)$ for h_d equal to 3 mm. Both methods are activated by a damage on the opposite side of the surface where the measurements are taken, irrespective of the damage depth h_d. To measure the effect of diminishing the number of active sensors, the ratio between the distance of the computed maximum position of $DI(x,y)$ or $P(x,y)$ and the actual notch position and the radius R_a has been computed. In case of damage 1, Figure 4a, with the notch in a symmetric position on the x axis, WSM and TM are comparable when all sensors are working, however reducing their number cause TM to lose accuracy on positioning the damage, whereas WSM is less sensitive to the reduction. With only 4 active sensors, both methods can detect the presence of the defect but are inaccurate in its location up to an error of more 100 % for TM and around 55 % for WSM. In case the notch is in a generic position, Figure 4b, TM seems slightly more accurate than WSM with all the available sensors. However, reducing their number cause TM to lose the ability to track the position up to a positioning error of 80 %. WSM seems less susceptible to the number of sensors, although the ability to track the damage position diminishes as well, giving rise to an error of 50 %.

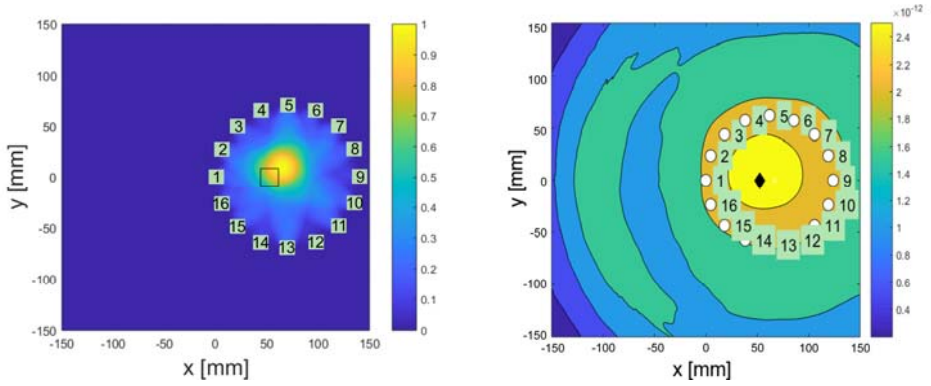

(a) *(b)*

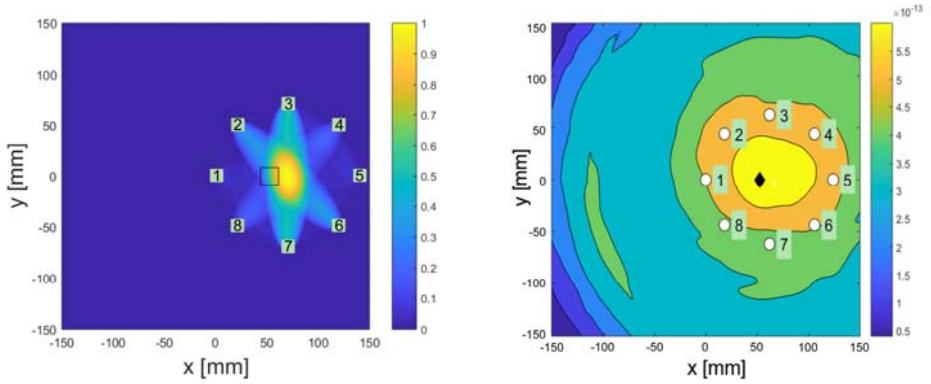

(c) *(d)*

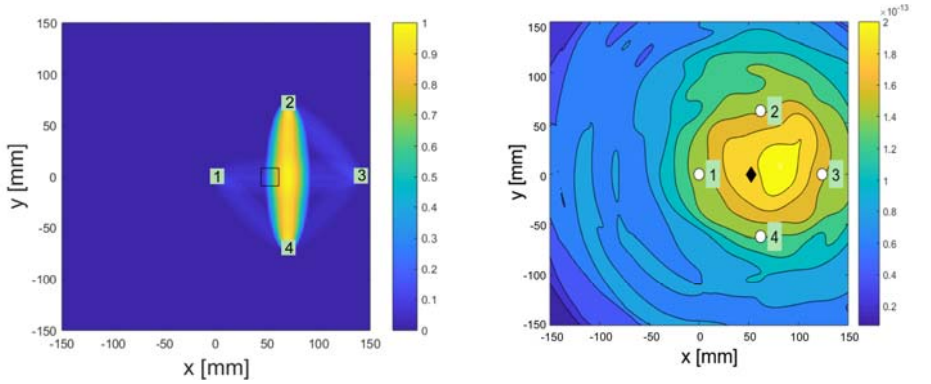

(e) *(f)*

Figure 2: Results for tomography with 16 (a) 8 (c) and 4 (e) sensor and for wave scattering with 16 (b) 8 (d) and 4 (f) sensors. Notch at (52.49, 0) mm and depth of 3 mm. Empty square denotes notch size and position whilst black diamonds only position.

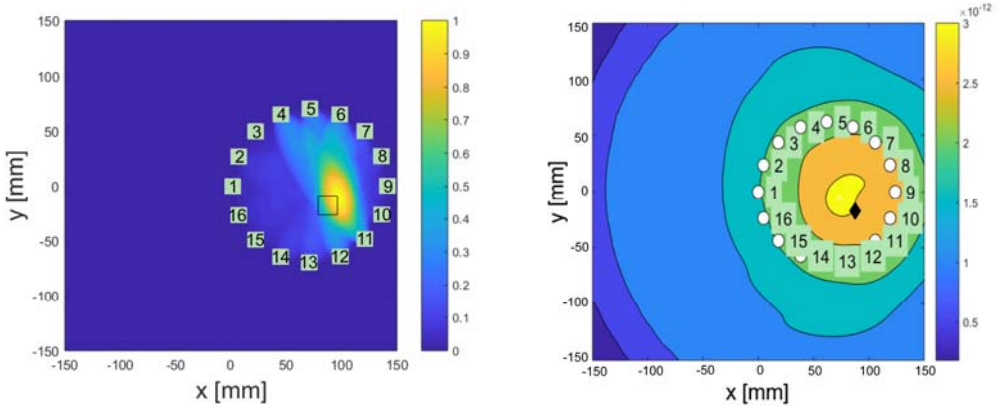

(a) *(b)*

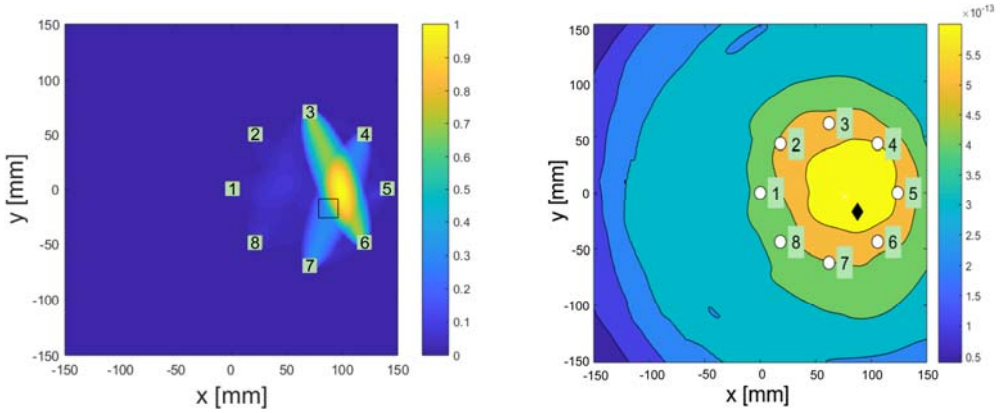

(c) *(d)*

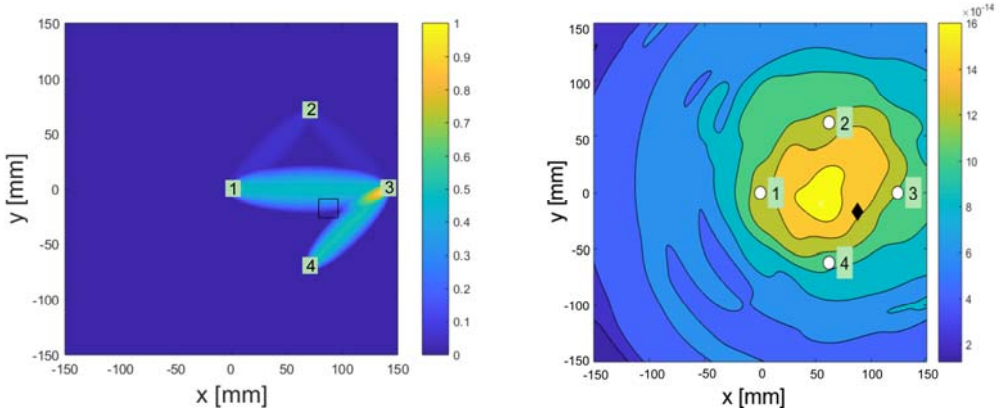

(e) *(f)*

Figure 3: Results for tomography with 16 (a) 8 (c) and 4 (e) sensor and for wave scattering with 16 (b) 8 (d) and 4 (f) sensors. Notch at (87.48, -17.50) mm and depth of 3 mm. Empty square denotes notch size and position whilst black diamonds only position.

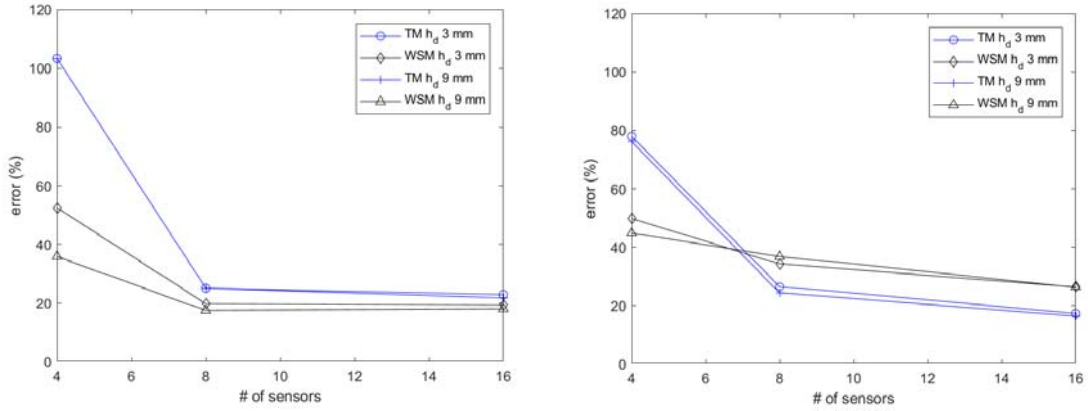

Figure 4: TM and WSM error for (a) damage 1 and (b) damage 2 test cases.

5. Conclusions

TM and WSM methods, with a full working array of 16 sensors, could detect the presence of a corrosion defect, irrespective of its depth; with a location error between 15 % to 30 %. Both methods have the desirable advantage to detect a corrosion defect located inside the tank, with the sensors positioned on the outside, even with a reduced number of working sensors, avoiding the necessity to empty the tank and to treat in a proper way its content during its inspection. In term of SHM, the sensibility of the methods to the number of active sensors is important: due to failures, one or more sensors can become inoperative. For both methods, a reduced number of active sensors does not affect the detection of the damage; on the other hand, its location is more dependent on the method and on the number of active sensors, with WSM more accurate than TM with a low number of active sensors. For a typical tank's life, the saving for checking its components health with both techniques could be relevant.

References

Bocchini P., Marzani A., Viola E., 2011, Graphical User Interface for guided acoustic waves, Journal of Computing in Civil Engineering 25(3), 202-210.

De Marchi L., Perelli A., Marzani A., 2013, A signal processing approach to exploit chirp excitation in Lamb wave defect detection and localization procedures, Mechanical Systems and Signal Processing, 39, 20-31.

Duczek S., Joulaian M., Düster A., Gabbert U., 2014, Numerical analysis of Lamb waves using the finite and spectral cell method, International Journal for Numerical Methods in Engineering, 99(1), 26–53.

Li X.X., Zhou S.Q., 2016, Assessing damages in pipes through circular distribution of ultrasonic guided wave reflections from defects, Chemical Engineering Transactions, 51, 541-546.

Maheri M.R., Abdollahi A., 2013, The effects of long term uniform corrosion on the buckling of ground based steel tanks under seismic loading, Thin-Walled Structures, 62, 1-9.

Monaco E., Boffa N.D., Memmolo V., Ricci F., Testoni N., De Marchi L., Marzani A., Hettler J., Tabatabaeipour M., Delrue S. Van Den Abeele K., 2016, Methodologies for Guided Wave-Based SHM System Implementation on Composite Wing Panels: Results and Perspective from SARISTU Scenario 5, Smart Intelligent Aircraft Structures (SARISTU), P.C. Wölcken and M. Papadopoulos (eds.), Springer International Publishing Switzerland

Shokrzadeh A.R., Sohrabi M.R., 2016, Buckling of ground based steel tanks subjected to wind and vacuum pressures considering uniform internal and external corrosion, Thin-Walled Structures,108, 333-350.

Tabatabaeipour M., Hettler J., Delrue S., Van Den Abeele K., 2014, 11th European Conference on Non-Destrutive Testing (ECNDT 2014), October 6-10, Prague, Czech Republic.

The MathWorks, Inc., 2017, MATLAB 9.2, Natick, Massachusetts, United States.

Willberg C., Duczek S., Vivar-Perez J.M., Ahmad Z.A.B., 2015, Simulation Methods for Guided Wave-Based Structural Health Monitoring: A Review, 67(1), 1-20.

Yan Zaho, Wenxiu Hao, Xiao Xu, 2017, Experimental study of the working stress state of concrete frame structures through ultrasonic testing, Chemical Engineering Transactions, 62, 919-924.